Chemosensory mechanisms of host seeking and infectivity in skin-penetrating nematodes

Spencer S. Gang[a,b,1], Michelle L. Castelletto[b], Emily Yang[a,b], Felicitas Ruiz[b], Taylor M. Brown[a,b,2], Astra S. Bryant[b], Warwick N. Grant[c], and Elissa A. Hallem[a,b,3]

[a]Molecular Biology Institute, University of California, Los Angeles, CA 90095; [b]Department of Microbiology, Immunology, and Molecular Genetics, University of California, Los Angeles, CA 90095; and [c]Department of Physiology, Anatomy, and Microbiology, La Trobe University, Bundoora 3086, Australia

Edited by L. B. Vosshall, The Rockefeller University, New York, NY, and approved June 8, 2020 (received for review June 5, 2019)

Approximately 800 million people worldwide are infected with one or more species of skin-penetrating nematodes. These parasites persist in the environment as developmentally arrested third-stage infective larvae (iL3s) that navigate toward host-emitted cues, contact host skin, and penetrate the skin. iL3s then reinitiate development inside the host in response to sensory cues, a process called activation. Here, we investigate how chemosensation drives host seeking and activation in skin-penetrating nematodes. We show that the olfactory preferences of iL3s are categorically different from those of free-living adults, which may restrict host seeking to iL3s. The human-parasitic threadworm *Strongyloides stercoralis* and hookworm *Ancylostoma ceylanicum* have highly dissimilar olfactory preferences, suggesting that these two species may use distinct strategies to target humans. CRISPR/Cas9-mediated mutagenesis of the *S. stercoralis tax-4* gene abolishes iL3 attraction to a host-emitted odorant and prevents activation. Our results suggest an important role for chemosensation in iL3 host seeking and infectivity and provide insight into the molecular mechanisms that underlie these processes.

parasitic helminth | parasitic nematode | *Strongyloides stercoralis* | host seeking | chemosensation

Skin-penetrating nematodes, including threadworms of the *Strongyloides* genus and hookworms of the *Ancylostoma* and *Necator* genera, are gastrointestinal parasites found primarily in tropical and subtropical regions around the world (1–3). Approximately 370 million people worldwide are infected with the threadworm *S. stercoralis* while ∼500 million people harbor hookworm infections from *Ancylostoma duodenale, Necator americanus*, or *A. ceylanicum* (4–7). These infections can lead to chronic intestinal distress, anemia, stunted growth and cognitive impairment in children, and in the case of *S. stercoralis*, death in immunosuppressed individuals (8, 9). Skin-penetrating nematodes exit an infected host as eggs or young larvae in host feces, and then develop in the environment on feces until they reach a developmentally arrested nonfeeding iL3 stage. The iL3 stage is developmentally similar to the dauer stage of free-living nematodes (10–12). iL3s navigate through the soil to find a host, a process called host seeking, and then breach the host's skin barrier. Inside the host, arrested iL3s undergo activation, an initial developmental progression whereby iL3s molt and resume feeding as they migrate toward the host's intestinal tract (13, 14). Host seeking and activation represent critical steps toward successful host infection, but the mechanisms underlying these behaviors and developmental processes are poorly understood.

Different skin-penetrating species only infect a narrow range of mammalian hosts (5, 15–18). For example, *S. stercoralis* naturally infects humans, primates, and dogs, while the closely related species *Strongyloides ratti* infects rats (Fig. 1*A*) (16, 17). It has long been hypothesized that iL3s find and infect hosts using host-emitted cues (19). Supporting this hypothesis, the iL3s of many parasitic nematode species engage in host-seeking behaviors in the presence of host-emitted olfactory, thermosensory, and gustatory cues, suggesting important roles for different sensory pathways in directing iL3s toward hosts in the environment (20–22). After finding and entering a host, iL3s also rely on the presence of host cues to trigger activation and resume development (13, 14, 23–31).

Host-emitted chemosensory cues are generally species specific and, thus, are likely to be important for the ability of iL3s to distinguish hosts from nonhosts. However, the chemosensory behaviors of mammalian-parasitic nematodes remain poorly understood. In particular, remarkably little is known about the chemosensory behaviors of hookworms, despite their worldwide prevalence. How the chemosensory preferences of iL3s differ from those of the noninfective environmental life stages, which have very different ethological requirements, also remains poorly understood. Furthermore, the molecular mechanisms underlying sensory-driven host-seeking and host-infection behaviors have been largely unexplored due to the long-standing genetic intractability of these parasites (32).

The human-infective nematode *S. stercoralis* is uniquely suited for mechanistic studies of human-parasitic behaviors. *S. stercoralis* and closely related species are exceptional among parasitic nematodes because they can develop through a complete free-living generation outside the host (Fig. 1*B*) (16). Adults isolated

ECOLOGY

Significance

Skin-penetrating nematodes are a major cause of morbidity worldwide. The infective larvae of these parasites actively search for humans to infect, but how they do this is poorly understood. We show that infective larvae have chemosensory preferences that are distinct from those of noninfective adults, which may ensure that only infective larvae host seek. We find that human-parasitic hookworms and threadworms have highly divergent chemosensory behaviors, suggesting they may use distinct strategies for finding and infecting humans. Finally, we show that the *S. stercoralis tax-4* gene is required for attraction to a human-emitted odorant and in-host development. Our results suggest that chemosensory pathways mediated by *Ss-tax-4* are important for the ability of infective larvae to find and infect human hosts.

Author contributions: S.S.G. and E.A.H. designed research; S.S.G., M.L.C., E.Y., F.R., and T.M.B. performed research; S.S.G., A.S.B., and W.N.G. contributed new reagents/analytic tools; S.S.G. and E.A.H. analyzed data; and S.S.G. and E.A.H. wrote the paper.

The authors declare no competing interest.

This article is a PNAS Direct Submission.

Published under the PNAS license.

Data deposition: The source code used in this paper is available on GitHub, https://github.com/HallemLab/Chemotaxis_Tracker.

[1]Present address: Division of Biological Sciences, University of California San Diego, La Jolla, CA 92093.

[2]Deceased December 12, 2019.

[3]To whom correspondence may be addressed. Email: ehallem@ucla.edu.

This article contains supporting information online at https://www.pnas.org/lookup/suppl/doi:10.1073/pnas.1909710117/-/DCSupplemental.

First published July 10, 2020.

Downloaded at Palestinian Territory, occupied on December 6, 2021

www.manaraa.com

A

Nematode species	Host range
S. stercoralis	Humans, primates, dogs
S. ratti	Rats
P. trichosuri	Brushtail possums
Graph legend	○ Free-living adults ● iL3s

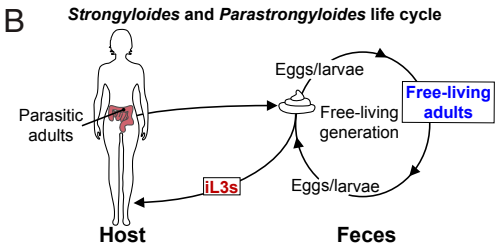

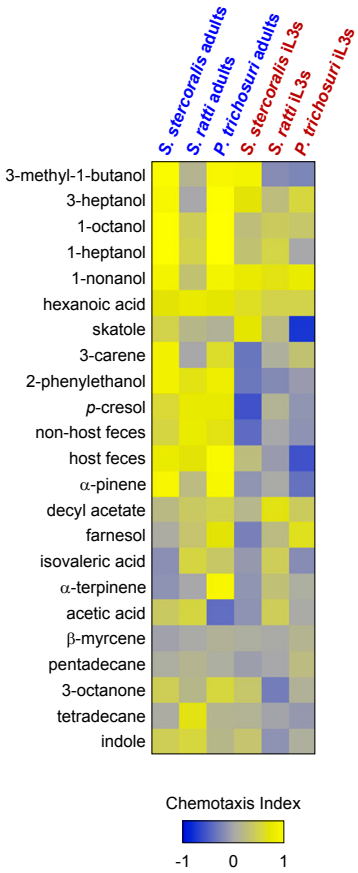

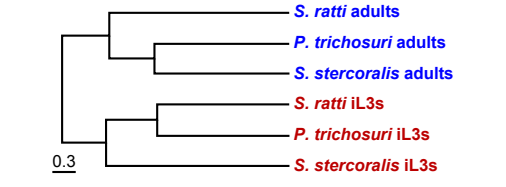

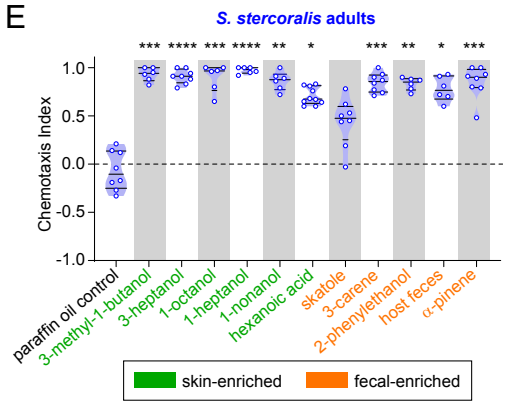

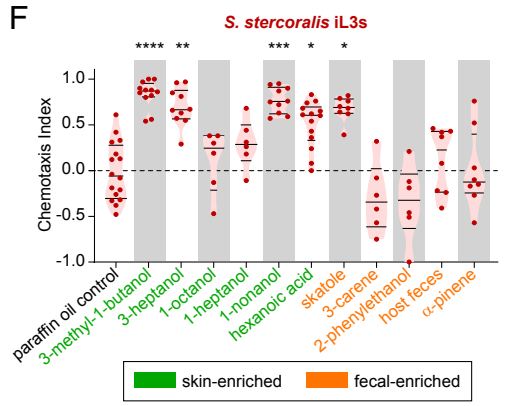

Fig. 1. Skin-penetrating nematodes display life-stage-specific olfactory preferences. (*A*) Summary of nematodes, their natural host ranges, and life stages tested. In *A*–*F*, the life stages tested are color coded: blue: free-living adults and red: iL3s. (*B*) The life cycle and ecology of *Strongyloides* and *Parastrongyloides*. Parasitic adults live in the host's intestinal tract and excrete eggs or young larvae in host feces. The larvae develop on host feces into free-living adult males and females. Progeny from free-living adults become iL3s that must infect a host to continue the life cycle. *S. stercoralis* and *S. ratti* can only undergo one free-living generation in the environment; all progeny from free-living adults become iL3s. *P. trichosuri* can cycle through multiple free-living generations in the environment while intermittently producing iL3s. (*C*) Responses of skin-penetrating nematodes to mammalian skin, sweat, and fecal odorants, as well as to host and nonhost fecal odors, across life stages. Sources of host and nonhost feces, respectively, for each species: *S. stercoralis*: dogs and rats; *S. ratti*: rats and dogs; *P. trichosuri*: brushtail possums and rats. Response magnitudes in the heatmap are color coded according to the scale shown below the heatmap. Odorants are ordered based on hierarchical cluster analysis. n = 6–20 trials for each odorant, species, and life stage combination. Each species and life stage responded differently to the odorant panel (****$P < 0.0001$, two-way ANOVA with Tukey's posttest). A subset of the data for *S. ratti* and *S. stercoralis* is from Castelletto et al. (37). (*D*) Olfactory preferences of skin-penetrating nematodes reflect life stage rather than phylogeny. The behavioral dendrogram was constructed based on the odorant response profiles in *C*. Hierarchical clustering was performed using the unweighted pair group method with arithmetic mean. Euclidean distance was used as a similarity measure (cophenetic correlation coefficient = 0.88). (*E* and *F*) Responses of *S. stercoralis* free-living adults (*E*) and iL3s (*F*) to selected odorants and feces. *$P < 0.05$, **$P < 0.01$, ***$P < 0.001$, and ****$P < 0.0001$. n = 6–16 trials for each odorant. Significance was calculated relative to the paraffin oil (PO) control using the full panel shown in *C*, Kruskal–Wallis test with Dunn's posttest. All odorant responses from the odorant panel that were significantly different from the PO control for either *S. stercoralis* adults or *S. stercoralis* iL3s are shown. Each dot represents an individual chemotaxis assay. Lines indicate medians and interquartile ranges. Odorants primarily considered human skin and sweat odorants are shaded green; odorants primarily considered human fecal odorants are shaded orange (*SI Appendix*, Table S1).

Downloaded at Palestinian Territory, occupied on December 6, 2021
www.manaraa.com

from this free-living generation are amenable to transgenesis and CRISPR/Cas9-mediated mutagenesis using techniques adapted from the model nonparasitic nematode *Caenorhabditis elegans* (33–35). Other parasitic nematodes, such as hookworms, are not yet amenable to CRISPR/Cas-mediated genetic engineering. Furthermore, *S. stercoralis* iL3s engage in robust sensory-driven behaviors, including chemotaxis toward host-emitted olfactory and gustatory cues, thermotaxis toward mammalian body temperatures, and activation in the presence of host cues (14, 36–42). Thus, *S. stercoralis* represents a powerful genetically tractable model to investigate the sensory-driven behaviors of skin-penetrating nematodes.

Here, we investigated the chemosensory mechanisms involved in host seeking and activation. We first conducted an in-depth analysis of olfactory preferences across life stages by examining how *S. stercoralis* iL3s and free-living adults respond to a large panel of mammalian-emitted odorants. The behaviors of *S. stercoralis* iL3s and adults were compared to those of iL3s and adults from two other closely related nematode species with similar life cycles but different host ranges, *S. ratti* and *Parastrongyloides trichosuri*. We found that the adults and iL3s of all three species exhibit both species-specific and life-stage-specific olfactory preferences. Specifically, the olfactory preferences of *S. stercoralis* iL3s more closely resembled those of *S. ratti* and *P. trichosuri* iL3s than *S. stercoralis* adults. This suggests that life stage is a major determinant of olfactory preferences and that olfaction may be an important contributor to life-stage-specific behaviors. We then asked how the olfactory preferences of *S. stercoralis* iL3s compare to those of the human-parasitic skin-penetrating hookworm *A. ceylanicum*. We found that *S. stercoralis* and *A. ceylanicum* iL3s show dramatic differences in odor-driven host seeking and environmental dispersal, raising the possibility that human-parasitic threadworms and hookworms use distinct strategies for finding and infecting hosts. We next investigated the molecular mechanisms that drive host seeking. We found that iL3s with CRISPR/Cas9-mediated disruption of the cGMP-gated cation channel subunit gene *tax-4* were unable to chemotax toward a host odorant, suggesting that host-seeking behavior involves cGMP signaling. Finally, we investigated the host-emitted sensory cues required for activation in *S. stercoralis*. We found that both CO_2 and 37 °C are critical cues for *S. stercoralis* activation. Moreover, *S. stercoralis tax-4* iL3s were unable to activate, indicating that cGMP signaling is required for activation. Our results provide molecular insights into the chemosensory pathways used by skin-penetrating iL3s for finding and infecting hosts.

Results

Olfactory Preferences Reflect Life-Stage-Specific Ecological Requirements. The odorant blends emitted by mammals are highly species specific (43, 44). Therefore, sensing host-emitted odorants could be an important way for iL3s to differentiate host from nonhost mammals (19). All skin-penetrating species have both infective and noninfective life stages present in the environment (20). This raises the question of which odorant cues might be specifically important for iL3s to locate hosts, and by contrast, which odorant cues might be beneficial for noninfective life stages to survive in the environment. To address this question, we examined the olfactory preferences of *S. stercoralis* free-living adults and iL3s. We then compared their odorant-driven behaviors to those of two additional species: the rat-parasitic nematode *S. ratti* and the nematode parasite of Australian brushtail possums *P. trichosuri* (Fig. 1*A*) (17, 45). We focused on *S. ratti* and *P. trichosuri* because, like human-infective *S. stercoralis*, they can undergo complete free-living generations in the environment before becoming iL3s that must infect a host (Fig. 1*B*). For *S. stercoralis* and *S. ratti*, the free-living cycle is restricted to one generation before all progeny become iL3s (16). In contrast, under favorable conditions, *P. trichosuri* can undergo many generations in the environment while intermittently producing iL3s and may represent an evolutionary intermediate between facultative and obligate parasitism (45–47). Together, the distinctive life cycles represented in the *Strongyloides* and *Parastrongyloides* genera offered an opportunity to investigate how olfactory preferences change between infective and noninfective life stages and across closely related species with different host ranges.

To assess olfactory preferences across different life stages, we asked how free-living adults and iL3s of each skin-penetrating species respond to a large panel of mammalian-associated odorants that includes odorants found in human skin, sweat, and feces (*SI Appendix*, Table S1). We also examined responses to mammalian fecal odor. Odorant preferences for each species and life stage were assessed using a chemotaxis assay (*SI Appendix*, Fig. S1) (37, 48). We found that each species and life stage tested against the mammalian-odorant panel exhibited a unique response profile (Fig. 1*C*). We then quantitatively compared the odor response profiles of *S. stercoralis*, *S. ratti*, and *P. trichosuri* iL3s and adults and found that the iL3s of each species had more similar odorant responses than any did to their respective free-living adult life stages (Fig. 1*D*). Our results indicate that, irrespective of species, host, or obligate versus facultative parasitic lifestyle, the transition to the iL3 stage represents a dramatic shift in olfactory preferences.

What accounts for the life-stage-specific olfactory preferences we observed in skin-penetrating nematodes? *S. stercoralis* adults were broadly attracted to individual odorants commonly found in human skin, sweat, and feces (Fig. 1*E*). They were also attracted to the odor of host feces (Fig. 1*E*). In contrast, *S. stercoralis* iL3s were neutral to many of the odorants that are abundant in feces, such as 3-carene, 2-phenylethanol, and α-pinene (Fig. 1*F*). They were also neutral to fecal odor (Fig. 1*F*). Attraction for *S. stercoralis* iL3s was limited to a subset of host-emitted skin and sweat odorants, although some of these odorants are also emitted from feces at low concentrations (Fig. 1*F* and *SI Appendix*, Fig. S2 and Table S1). Similar shifts from attraction to fecal odor and odorants at the free-living adult stage to reduced or no attraction at the iL3 stage were also observed in *S. ratti* and *P. trichosuri* (*SI Appendix*, Figs. S3 and S4). We note that, initially, iL3 chemotaxis was tested using undiluted point sources of odorant, while free-living adult chemotaxis was tested using 1:10 odorant dilutions since some undiluted odorants were toxic to free-living adults. To confirm that life-stage-specific changes in olfactory preferences were a result of the life-stage transition and not an odorant concentration effect, we tested *S. stercoralis* iL3s at 1:10 dilutions for selected odorants and observed similar differences in behavior between adults and iL3s (*SI Appendix*, Fig. S5). Thus, the shift from odorant attraction at the adult stage to neutrality at the iL3 stage represents a change in olfactory preferences, not a concentration effect.

Together our results raise the possibility that the free-living life stages may be retained on host feces at least in part by their robust attraction to host fecal odor, despite their attraction to skin and sweat odorants. Feces represent a bacteria-rich food source where the nematodes can grow, reproduce, and generate large populations of iL3 progeny. At the nonfeeding developmentally arrested iL3 stage, attraction to fecal odor is down-regulated, which may promote the dispersal of iL3s into the environment in search of hosts. Our observations are consistent with a previous study that tested a small panel of host-emitted odorants across life stages (37). We hypothesize that the odorants that remain attractive at the iL3 stage may be those that are important for host seeking.

Human-Infective *S. stercoralis* and *A. ceylanicum* Have Distinct Olfactory Preferences. Both threadworms and hookworms infect by skin penetration and target some of the same host species. However, they are evolutionarily distant and are phylogenetically grouped into distinct clades (47, 49). To date, there has been

ECOLOGY

Downloaded at Palestinian Territory, occupied on December 6, 2021

www.manaraa.com

little direct investigation of the similarities or differences by which threadworms and hookworms target human hosts. Furthermore, even though human-infective hookworms are a major source of neglected tropical disease, remarkably little is known about their olfactory behaviors.

To evaluate the odor-driven behaviors of threadworms and hookworms in detail, we directly compared the olfactory preferences of *A. ceylanicum*, a common parasite of carnivores in Southeast Asia that can also infect humans, and *S. stercoralis* (Fig. 2*A*) (5). Unlike *S. stercoralis*, hookworm species, such as *A. ceylanicum*, lack a free-living generation; instead, eggs excreted from the host develop through two larval stages in the environment before developing into iL3s (Fig. 2*B*). We assessed how *A. ceylanicum* iL3s respond to the panel of host-emitted odorants and compared their responses to those of *S. stercoralis* iL3s. Surprisingly, we found that *A. ceylanicum* iL3s had dramatically different olfactory preferences compared to *S. stercoralis* iL3s (Fig. 2*C*). *A. ceylanicum* iL3s were attracted to feces, the fecal-odorant 2-phenylethanol, and the sebum-enriched odorant farnesol (Fig. 2*D* and *SI Appendix*, Fig. S6). By contrast, *S. stercoralis* iL3s were neutral to these odorants and, instead, preferred odorants more prevalently emitted from skin and sweat (Figs. 1*F* and 2*E*).

The divergent olfactory preferences of hookworms and threadworms raise the possibility that these two human-parasitic species employ very different strategies for host seeking. Intriguingly, *A. ceylanicum* iL3s infect by both oral and skin penetration routes, while *S. stercoralis* is thought to infect mainly by skin penetration (5, 16, 50). Therefore, it is possible that infection mode shapes the odor-driven behaviors of parasitic nematodes. For *S. stercoralis*, favoring skin and sweat odorants may be important for iL3 fitness since locating host skin is critical for successful infection. In contrast, *A. ceylanicum* iL3s may be less dependent on attraction to host skin because it is not the only route for host invasion.

***S. stercoralis* and *A. ceylanicum* iL3s Have Different Dispersal Behaviors.** The contrasting chemotactic responses of *S. stercoralis* and *A. ceylanicum* iL3s to host fecal odor and individual odorants prevalent in host feces raised the question of whether these species have different environmental dispersal strategies. To investigate this question, we examined the tendency of *S. stercoralis* and *A. ceylanicum* iL3s to disperse from host feces using fecal dispersal assays (51). We placed iL3s on uninfected feces from permissive laboratory hosts (referred to hereafter as "host feces") for each species (52, 53) and monitored the frequency with which iL3s migrated away from the fecal pellet (Fig. 3*A*). We found that, on average, ∼60% of *S. stercoralis* iL3s but only 30% of *A. ceylanicum* iL3s migrated off of the fecal pellet (Fig. 3 *B*, *Left*). Furthermore, for *A. ceylanicum*, of the 30% of iL3s that left the fecal pellet, the majority of those individuals stayed near the feces; only ∼10% of the iL3s migrated to the outermost zone of the assay plate (Fig. 3 *B*, *Right*). By contrast, over 50% of all *S. stercoralis* iL3s migrated to the outer zone (Fig. 3 *B*, *Right*). The basal crawling speeds of *S. stercoralis* and *A. ceylanicum* are similar (40), suggesting that these differences reflect differences in dispersal strategy rather than crawling speed. However, to further ensure that our dispersal results are independent of crawling speed, we repeated the dispersal assay using a 3-h assay instead of a 1-h assay. We found that the results from a 3-h assay were similar to those from a 1-h assay: *S. stercoralis* iL3s dispersed from feces more than *A. ceylanicum* iL3s (*SI Appendix*, Fig. S7*A*). Together, these results suggest that *S. stercoralis* iL3s may disperse from feces and into the surrounding environment to a greater extent than *A. ceylanicum* iL3s.

To test whether dispersal behavior is regulated by host-species-specific factors in the feces, we then examined the dispersal of both nematodes from feces of the same nonhost species, the rat. Similar to our results with host feces, *S. stercoralis* iL3s dispersed more from rat feces than *A. ceylanicum* iL3s (*SI Appendix*, Fig. S7*B*). These results suggest that species-specific factors in feces are not major determinants of dispersal behavior. Instead, the different dispersal tendencies of *S. stercoralis* versus *A. ceylanicum* iL3s appear to be due to factors intrinsic to the nematodes.

To further compare the dispersal behaviors of *S. stercoralis* and *A. ceylanicum*, we examined their nictation behaviors. Nictation is a strategy employed by many parasitic nematode species whereby the infective larva elevates its body and waves itself above a surface in an attempt to facilitate attachment to a passing host (20, 37). We previously found that *S. stercoralis* iL3s exhibit low nictation frequencies and, instead, prefer to crawl (37). Here, we tested *S. stercoralis* and *A. ceylanicum* iL3 nictation in parallel using an "artificial dirt" agar chip (51, 54). The chip consisted of an evenly spaced array of near-microscopic agar posts arranged such that the iL3s could crawl between the posts on the agar surface or could crawl up the agar posts to nictate (Fig. 3*C*). We quantified nictation frequencies for both species and found that *A. ceylanicum* iL3s nictated at higher rates than *S. stercoralis* iL3s. Approximately 50% of *A. ceylanicum* iL3s nictated during a 2-min observation period, while only 13% of *S. stercoralis* iL3s nictated under the same conditions (Fig. 3*D*). This difference in nictation frequency is not the result of differences in iL3 length since a comparison of nictation frequencies across multiple nematode species revealed no significant correlation between nictation frequency and iL3 length (*SI Appendix*, Fig. S8). Together, the observations that *A. ceylanicum* iL3s are attracted to fecal odorants, tend to stay on or near host feces, and frequently nictate suggest that many of the iL3s may wait for potential hosts to pass by fecal deposits before engaging in host-seeking behaviors. In contrast, *S. stercoralis* iL3s may be more likely to migrate off feces and actively search for hosts to infect.

***S. stercoralis tax-4* Is Required for Odor-Driven Host Seeking.** To date, remarkably little is known about the molecular basis for chemosensation in parasitic nematodes. However, the molecular mechanisms underlying chemosensation in *C. elegans* are well characterized (55). In *C. elegans*, the cyclic-nucleotide-gated heterodimeric channel TAX-4/TAX-2 is required for sensory transduction in many sensory neurons, including the AWB and AWC olfactory neurons (55–57). Moreover, in the plant-parasitic nematode *Meloidogyne incognita*, knockdown of *Mi-tax-2* and *Mi-tax-4* by RNAi results in chemotaxis defects (58). We previously identified the *S. stercoralis* homolog of the *C. elegans tax-4* gene, disrupted its function with CRISPR/Cas9-mediated mutagenesis, and demonstrated that *Ss-tax-4* is required for temperature-driven host seeking in *S. stercoralis* iL3s (34, 40). To test whether *Ss-tax-4* also plays a role in odor-driven host seeking, we first examined how *S. stercoralis* iL3s respond to the skin and sweat odorant 3-methyl-1-butanol (hereafter 3m1b, also referred to as isoamyl alcohol) using a single iL3 chemotaxis assay (48). The odorant 3m1b was selected because it is one of the most attractive host-emitted odorants identified for *S. stercoralis* iL3s (Fig. 1 *C* and *F*) (37).

We collected *S. stercoralis* wild-type iL3s and imaged the real-time migration of individual animals in a modified chemotaxis assay where the iL3 was given a choice between 3m1b and the paraffin oil (PO) diluent (*SI Appendix*, Fig. S9*A*). Wild-type iL3s preferred to navigate toward 3m1b over the PO control (*SI Appendix*, Fig. S9*B* and Movie S1). In contrast, the PO alone did not elicit a directional behavioral response (*SI Appendix*, Fig. S9*C* and Movie S2). Thus, individual wild-type iL3s were significantly more likely to navigate toward 3m1b than toward PO (*SI Appendix*, Fig. S9*D*) and spent more time dwelling near 3m1b than near PO (*SI Appendix*, Fig. S9*E*).

We next asked if *Ss-tax-4*-mediated signal transduction contributes to this behavior by disrupting *Ss-tax-4* using CRISPR/Cas9-mediated

Downloaded at Palestinian Territory, occupied on December 6, 2021
www.manaraa.com

A

Nematode species	Host range	Infection mode
A. ceylanicum	Humans, South Asian carnivores	Skin penetration, passive ingestion
S. stercoralis	Humans, primates, dogs	Skin penetration
Graph legend	● *A. ceylanicum* iL3s	○ *S. stercoralis* iL3s

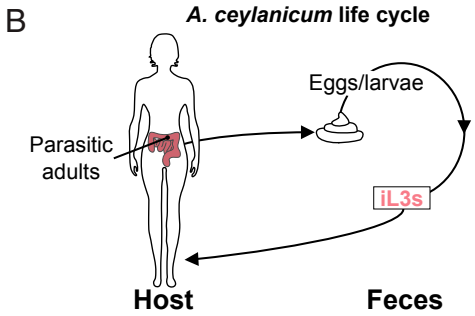

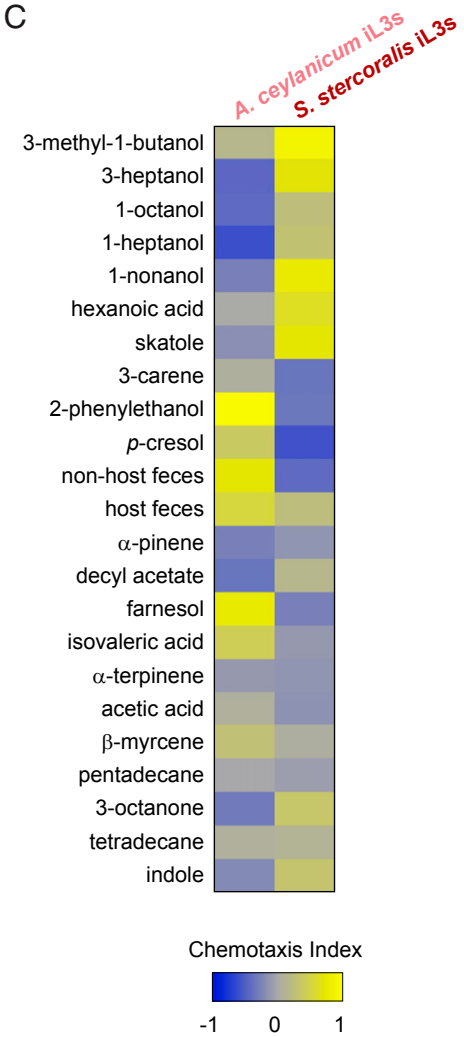

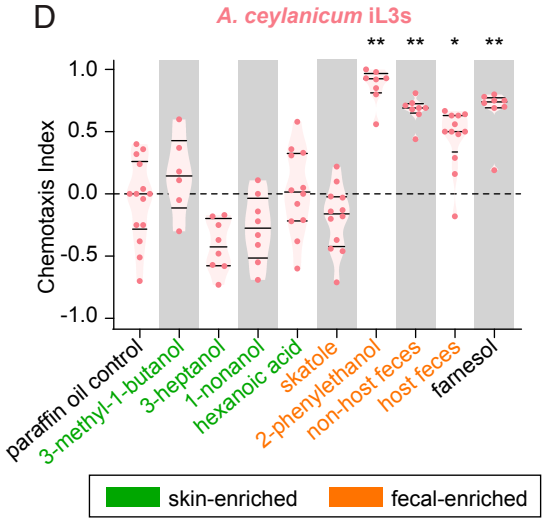

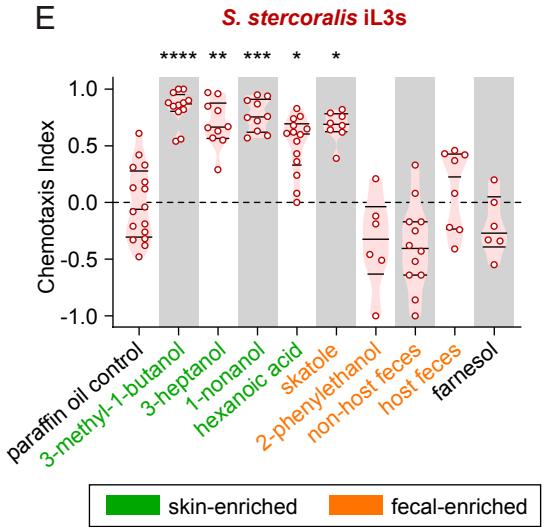

Fig. 2. The human-infective species *A. ceylanicum* and *S. stercoralis* have distinct olfactory preferences. (*A*) Summary of natural host ranges, infection modes, and life stages tested for the hookworm *A. ceylanicum* and the threadworm *S. stercoralis*. In *A*–*E*, the species are color coded: pink: *A. ceylanicum* iL3s and red: *S. stercoralis* iL3s. (*B*) The life cycle and ecology of *A. ceylanicum*. Parasitic adults excrete eggs in host feces. *A. ceylanicum* larvae can only develop into iL3s that must infect a new host each generation. (*C*) Responses of *A. ceylanicum* iL3s and *S. stercoralis* iL3s to mammalian skin, sweat, and fecal odorants, as well as to host and nonhost fecal odors. Sources of host and nonhost feces, respectively, for each species: *A. ceylanicum*: hamsters and gerbils; *S. stercoralis*: dogs and rats. Response magnitudes are color coded according to the scale shown below the heatmap. Odorants are shown in the same order as in Fig. 1. $n = 6$–16 trials for each odorant and species combination. *A. ceylanicum* and *S. stercoralis* responded differently to the odorant panel (****$P < 0.0001$, two-way ANOVA with Tukey's posttest). (*D* and *E*) Responses of *A. ceylanicum* iL3s (*D*) and *S. stercoralis* iL3s (*E*) to selected odorants and fecal odor. *$P < 0.05$, **$P < 0.01$, ***$P < 0.001$, and ****$P < 0.0001$. $n = 6$–16 trials for each odorant for both *A. ceylanicum* and *S. stercoralis* iL3s. Significance was calculated relative to the PO control using the full panel shown in *C*, Kruskal–Wallis test with Dunn's posttest. All odorant responses from the odorant panel that were significantly different from the PO control for either *A. ceylanicum* iL3s or *S. stercoralis* iL3s are shown. Each dot represents an individual chemotaxis assay. Lines indicate medians and interquartile ranges. Odorants primarily considered human skin and sweat odorants are shaded green; odorants primarily considered human fecal odorants are shaded orange (*SI Appendix*, Table S1). Data for *S. stercoralis* iL3s are reproduced from Fig. 1.

Downloaded at Palestinian Territory, occupied on December 6, 2021

المنارة للاستشارات
www.manaraa.com

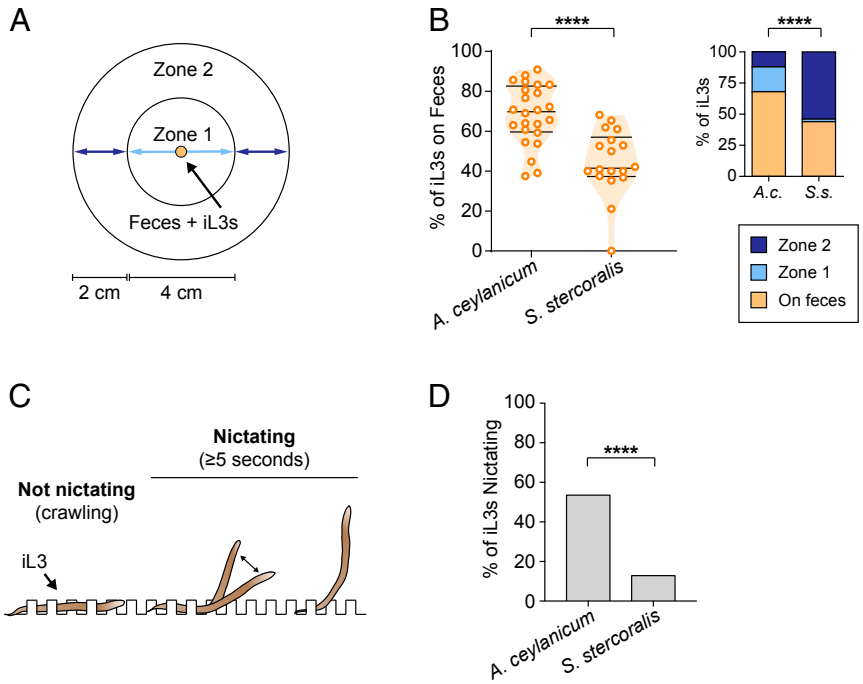

Fig. 3. *A. ceylanicum* and *S. stercoralis* have distinct dispersal behaviors. (*A*) Diagram of the fecal dispersal assay for iL3s. iL3s were placed on fresh host feces (hamster feces for *A. ceylanicum* and gerbil feces for *S. stercoralis*) and were allowed to migrate for 1 h. The number of iL3s on feces, in zone 1, or in zone 2 was then quantified. The diagram was modified from Ruiz et al. (51). (*B*, *Left*) Percentage of iL3s remaining on feces at the end of the 1-h fecal dispersal assay for *A. ceylanicum* and *S. stercoralis*. *S. stercoralis* iL3s disperse off feces to a greater extent than *A. ceylanicum* iL3s. ****$P < 0.0001$, Mann–Whitney test. $n = 18$ trials for *S. stercoralis* and 24 trials for *A. ceylanicum*. Each dot represents an individual fecal dispersal assay. Lines indicate medians and interquartile ranges. (*Right*) Percentage of iL3s in each zone at the end of the 1-h fecal dispersal assay. The overall distribution of iL3s differed between species. ****$P < 0.0001$, χ^2 test. Moreover, the distribution of iL3s on feces, in zone 1, and in zone 2 all significantly differed between *A. ceylanicum* and *S. stercoralis* iL3s ($P < 0.001$, Fisher's exact test with Bonferroni correction). $n = 367$ iL3s for *S. stercoralis* and 605 iL3s for *A. ceylanicum*. (*C*) Diagram of the nictation assay for iL3s. iL3s were placed on near-microscopic agar posts where they could crawl between posts or nictate on the posts. Individual iL3s were monitored for a 2-min period. Any iL3 that raised at least half its body off the plate for ≥5 s was scored as nictating. The diagram was modified from Ruiz et al. (51). Post heights and the iL3 size shown are not to scale. (*D*) *A. ceylanicum* iL3s nictated more frequently than *S. stercoralis* iL3s. ****$P < 0.0001$, Fisher's exact test. $n = 62$ iL3s for *S. stercoralis* and 71 iL3s for *A. ceylanicum*.

targeted mutagenesis. We generated *S. stercoralis* iL3s with homology-directed insertion of an *mRFPmars* reporter gene encoding a red fluorescent protein at the *Ss-tax-4* target locus (*SI Appendix*, Fig. S10 *A* and *B*) (34, 40). Candidate transgenic animals were tested in the single iL3 chemotaxis assay and then genotyped post hoc for homozygous disruption of *Ss-tax-4* (Fig. 4*A* and *SI Appendix*, Fig. S10 *B–D* and Tables S2–S4). As a control, we performed our CRISPR/Cas9 approach but omitted the Cas9 construct to generate "no-Cas9-control" iL3s that expressed *mRFPmars* but lacked disruption of the *Ss-tax-4* gene (34, 40). No-Cas9-control worms were tested in the single iL3 chemotaxis assay and genotyped post hoc to confirm that homology-directed repair did not occur at the *Ss-tax-4* locus. As observed with wild-type iL3s, individual no-Cas9-control iL3s tested in the 3m1b versus PO chemotaxis assay consistently migrated toward 3m1b (Fig. 4*B* and Movie S3). In contrast, *Ss-tax-4* iL3s showed no preference for 3m1b over PO. They were significantly less likely to migrate toward 3m1b or dwell near the 3m1b than no-Cas9-control iL3s (Fig. 4 *C–E* and Movie S4). Thus, functional signal transduction through *Ss-tax-4*-dependent pathways appears to be critical for the migration of *S. stercoralis* iL3s toward a host-emitted odorant.

Heat and CO_2 Are Required for Activation of *S. stercoralis* iL3s. Locating a host in the environment is only the first step for skin-penetrating nematodes to successfully establish an infection. Following skin penetration, iL3s activate: They resume feeding and reinitiate development inside the host. The transition from the soil to inside a host represents a dramatic change in environment for iL3s, and iL3s are thought to use chemosensory mechanisms to detect host factors and initiate activation upon host entry. Studies in a number of species have identified multiple host-associated cues that contribute to iL3 activation, including elevated temperature, high CO_2 levels, host serum, carbonic acid, and reduced glutathione (13, 14, 23–31). However, the specific requirement for each of these cues varies across species (13, 14, 23–31). In the case of *S. stercoralis*, iL3s were previously shown to efficiently activate in a 37 °C and 5% CO_2 environment in the presence of Dulbecco's modified Eagle medium (DMEM) tissue culture media, canine serum, and glutathione (14). Replacement of DMEM with buffered saline solution (BU) eliminated activation, suggesting an important role for inorganic salts, amino acids, pyruvate, glucose, or other host factors in iL3 activation (30, 31). However, the requirement for heat and CO_2 in *S. stercoralis* iL3 activation was not tested.

To directly test the requirement for heat and CO_2 in *S. stercoralis* activation, we used an in vitro activation assay (Fig. 5 *A* and *B*) (14). We found that ∼50% of *S. stercoralis* iL3s activated after 24 h in hostlike culture conditions including DMEM tissue culture media, 37 °C, and 5% CO_2 (Fig. 5*C*). We next asked if removal of either the elevated temperature or the 5% CO_2 from the culture conditions would change activation rates. We found that independently decreasing the temperature to 25 °C or providing a near-0% CO_2 environment (atmospheric CO_2 is ∼0.04% , ref. 59) dramatically reduced activation rates (Fig. 5*C*). These results were similar to those previously observed for

Downloaded at Palestinian Territory, occupied on December 6, 2021
www.manaraa.com

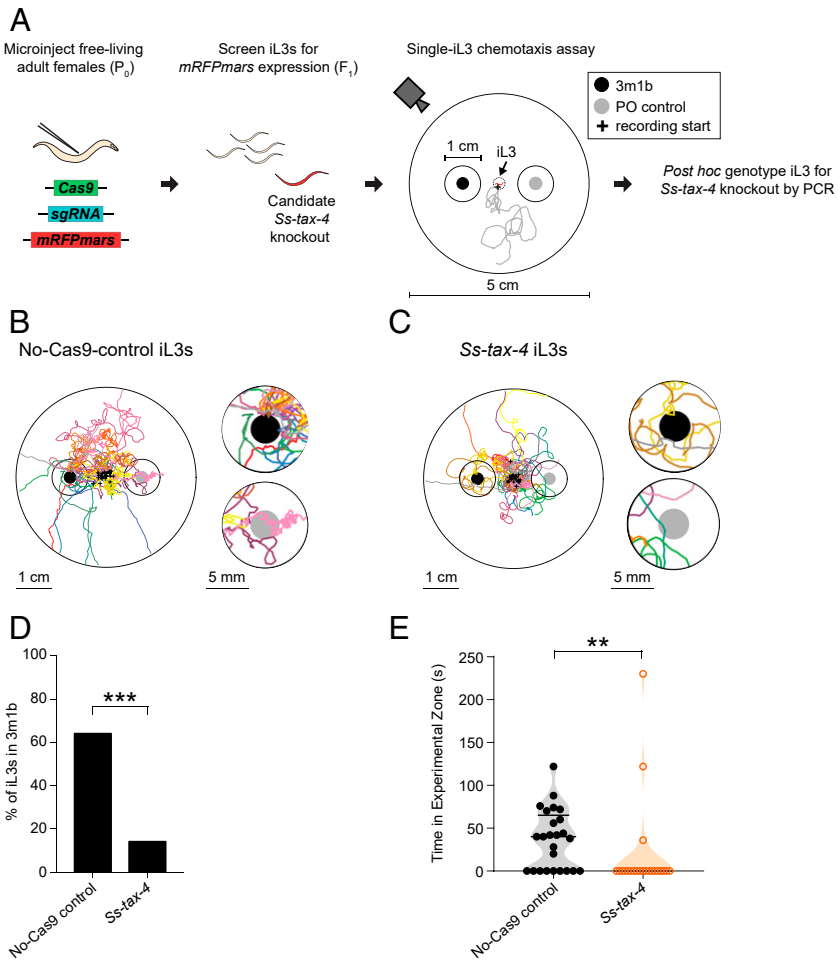

Fig. 4. *Ss-tax-4* is required for the attraction of *S. stercoralis* iL3s to a host odorant. (*A*) Strategy for CRISPR/Cas9-mediated targeted mutagenesis of the *S. stercoralis tax-4* gene. Plasmid vectors encoding Cas9, the single guide RNA for *Ss-tax-4*, and a repair template for homology-directed repair encoding an *mRFPmars* reporter gene were introduced into *S. stercoralis* free-living adult females by gonadal microinjection. The iL3 progeny from microinjected females were screened for *mRFPmars* expression, indicative of possible disruption of *Ss-tax-4*. Individual *mRFPmars*-expressing iL3s were then live tracked in a chemotaxis assay where the iL3 could crawl freely on an agar surface in an odorant gradient. Black dot: placement area of a 5-μL drop of a 1:10 dilution of the attractive odorant 3m1b in PO; gray dot: placement area of a 5-μL drop of PO; black circles around the dots: the experimental or control zones surrounding the 3m1b or PO, respectively. Gray line: hypothetical reconstruction of the migratory path of an *mRFPmars*-expressing iL3 in the chemotaxis assay; the plus sign indicates the starting position of the iL3. iL3s were then PCR genotyped post hoc for homozygous disruption of *Ss-tax-4* (*SI Appendix*, Fig. S10) as previously described (34, 40). (*B*) Tracks of no-Cas9-control iL3s migrating for ∼6 min or until the iL3 left the 5-cm assay arena in an odorant gradient. Each colored line indicates the migration of an independently tested iL3; the plus signs indicate the starting positions of the iL3s. The full assay arena is shown on the *Left*. An enlarged view of the scoring regions around the odorant and control are shown on the *Right*. Black dots, gray dots, and black circles are as defined above. (*C*) Tracks of *Ss-tax-4* iL3s migrating for ∼6 min or until the iL3 left the 5-cm assay arena in an odorant gradient, shown as described in *B*. (*D*) The percentage of no-Cas9-control and *Ss-tax-4* iL3s entering the 3m1b experimental zone; a larger percentage of no-Cas9-control iL3s enter the experimental zone than *Ss-tax-4* knockout iL3s. ***$P < 0.001$, Fisher's exact test. $n = 22$–25 iL3s for each assay condition. (*E*) The time spent by each iL3 in the experimental zone containing 3m1b for either no-Cas9-control iL3s or *Ss-tax-4* iL3s. No-Cas9-control iL3s spend more time in the experimental zone than *Ss-tax-4* iL3s. **$P < 0.01$, Mann–Whitney test. $n = 22$–25 iL3s for each assay condition.

in vitro activation of the canine hookworm *Ancylostoma caninum* (13), but the importance of a high-CO_2 environment on iL3 activation was more pronounced for *S. stercoralis*.

For these assays, activated versus nonactivated iL3s were identified based on their feeding status since resumption of feeding is an early indicator of activation. However, to control for the possibility that feeding but not activation might be specifically disrupted at lower temperatures, we repeated the assay using dispersal as a different measure of activation. Specifically, we compared the dispersal of unstimulated iL3s crawling on a plate at room temperature for two different iL3 populations: iL3s incubated for 24 h in DMEM at 37 °C with 5% CO_2 (the activation condition) and iL3s incubated in BU saline (26) at room temperature for 24 h in the absence of CO_2 (the control condition). If iL3s in the control condition had, in fact, activated, but their feeding behavior was specifically disrupted, we would expect no difference in the tendency of both populations to disperse. However, we found that iL3s subjected to the activation condition dispersed significantly less than iL3s exposed to the control condition (*SI Appendix*, Fig. S11). These results confirm that iL3s subjected to the control condition do not activate, and, therefore, that heat and CO_2 are required for activation.

Hostlike 37 °C and 5% CO_2 culture conditions were also required for in vitro activation of both *S. ratti* and *P. trichosuri* iL3s (*SI Appendix*, Fig. S12). Together our results demonstrate that elevated CO_2 in combination with 37 °C and gustatory cues from tissue culture media appear to be essential for activation in both *Strongyloides* species and *Parastrongyloides*.

ECOLOGY
Downloaded at Palestinian Territory, occupied on December 6, 2021
www.manaraa.com

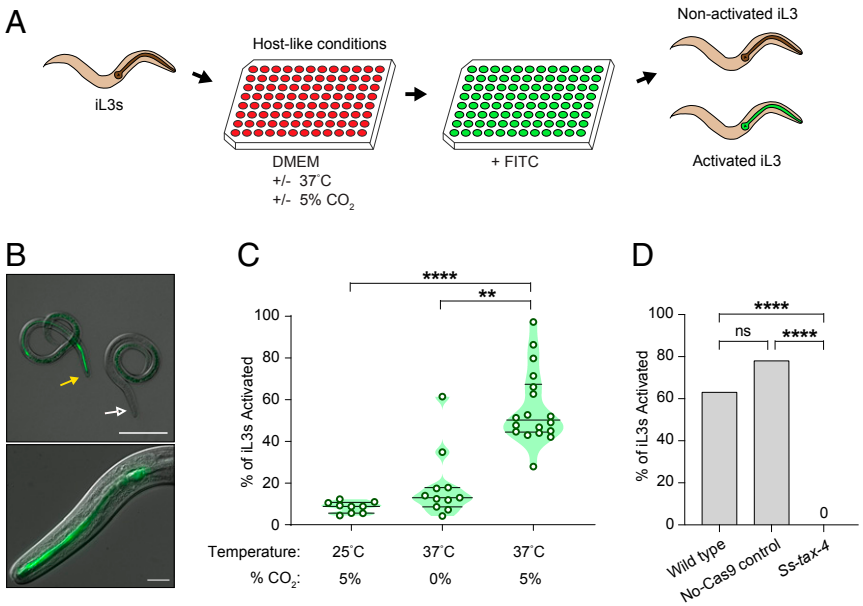

Fig. 5. *Ss-tax-4* is required for *S. stercoralis* iL3 activation. (*A*) Schematic of an in vitro assay for iL3 activation. Developmentally arrested iL3s are incubated in hostlike conditions in DMEM culture medium at 37 °C with 5% CO_2. After 21 h of incubation, fluorescein isothiocyanate (FITC) is added to the medium. Following a 3-h incubation with FITC, the iL3s are washed, anesthetized, plated, and screened for FITC in their pharynx. iL3s with FITC in their pharynx are scored as activated since ingestion of FITC is indicative of the resumption of feeding that occurs during activation. (*B*, *Top*) Representative DIC + epifluorescence overlay of an activated iL3 with FITC in the pharynx (closed yellow arrow) and an iL3 that failed to activate following 24 h of incubation (open white arrow). (Scale bar: 100 μm.) (*Bottom*) Magnified DIC + epifluorescence overlay of an activated iL3 with FITC in the pharynx. (Scale bar: 10 μm.) (*C*) Heat and CO_2 are required for activation of *S. stercoralis* iL3s. $^{**}P < 0.01$, $^{****}P < 0.0001$, Kruskal–Wallis test with Dunn's posttest. n = 9–18 trials per condition. Percentage of iL3s activated = number of FITC-positive activated iL3s/total number of iL3s scored. Green dots: % activation for each trial, ~100 iL3s scored per trial. Lines indicate medians and interquartile ranges. (*D*) Whereas wild-type and no-Cas9-control iL3s activate in hostlike conditions, CRISPR/Cas9-edited *Ss-tax-4* iL3s do not. $^{****}P < 0.0001$, χ^2 test with Bonferroni correction. n = 49 wild-type iL3s, 36 no-Cas9-control iL3s, and 30 *Ss-tax-4* iL3s.

***S. stercoralis tax-4* Is Required for Activation.** In *C. elegans,* the *tax-4* gene plays a role in regulating both entry into and exit from the dauer larval state (60, 61). To gain insight into the molecular mechanisms that mediate activation, we therefore asked if CRISPR/Cas9-mediated disruption of *Ss-tax-4* would alter activation rates. We found that, while individual wild-type iL3s and no-Cas9-control iL3s consistently activated in the presence of DMEM, 37 °C, and 5% CO_2, we never observed activation for any *Ss-tax-4* iL3s tested (Fig. 5*D*). Thus, *Ss-tax-4*-dependent pathways, which appear to be important for host seeking, also appear to be critical for iL3 activation. Our results identify a genetic pathway that may be required for skin-penetrating nematodes to initiate development following host entry.

Discussion

We conducted a large-scale quantitative analysis of the olfactory preferences of skin-penetrating nematodes, including two human-parasitic species, and identified life-stage-specific olfactory preferences that fit the distinct environmental needs of the different life stages. *S. stercoralis*, *S. ratti*, and *P. trichosuri* free-living adults were attracted to mammalian-emitted odorants prevalent in feces as well as fecal odor (Fig. 1 *C* and *E* and *SI Appendix*, Figs. S2–S4). Free-living adults and larvae feed on fecal bacteria (16). While skin-penetrating nematodes are capable of developing on *Escherichia coli*, their reproductive output when cultured on *E. coli* is greatly diminished relative to their reproductive output when cultured on the complex bacterial populations represented in mammalian feces (34, 35, 62). Therefore, attraction to host fecal odorants may contribute to the tendency of free-living life stages to stay on or near feces, which is maximally suited for their growth and reproduction. In contrast to free-living adults, iL3s have less incentive to remain on or near fecal deposits since they are nonfeeding. *Strongyloides* and *Parastrongyloides* appear to share a mechanism whereby attraction to fecal odorants is down-regulated in iL3s, which may contribute to the tendency of these iL3s to disperse into the environment (Fig. 1 *C* and *F* and *SI Appendix*, Figs. S2–S4) (37). These iL3s favor odorants that are likely to facilitate finding host skin, which is essential for their continued development.

The iL3s of the hookworm *A. ceylanicum* have olfactory preferences that are distinct from those of *S. stercoralis* iL3s, despite the fact that both species target humans (Fig. 2). Unlike *S. stercoralis* iL3s, *A. ceylanicum* iL3s displayed strong attraction to host feces and fecal odorants (Fig. 2). In addition, *A. ceylanicum* iL3s tended to disperse less from feces and had a higher propensity to nictate than *S. stercoralis* iL3s (Fig. 3). Our characterization of *A. ceylanicum* dispersal and nictation behaviors fits with previous observations that some hookworm species often wait in a motionless state and only begin locomotion when certain host-derived cues are in close proximity (63, 64). Taken together, the respective responses of hookworm and threadworm iL3s to feces and fecal odorants suggest there may be important differences in the host-seeking strategies used by these two species.

Like *A. ceylanicum* iL3s, iL3s of the passively ingested murine parasite *Heligmosomoides polygyrus* are also attracted to host feces (51). Fecal attraction is thought to retain some *H. polygyrus* iL3s on feces, where they are swallowed during coprophagy (51). Oral infection has been documented in many hookworm species, including *A. ceylanicum*, *A. duodenale*, and *N. americanus*; in some cases, it is thought to be a major infection route (5, 65, 66). In contrast, oral infection is thought to be less common in the case of *S. stercoralis* (50). Our results with *A. ceylanicum* raise the possibility that attraction to feces may be a general strategy employed by parasitic nematodes that infect orally, even if they rely on indirect fecal–oral transmission rather than coprophagy.

Downloaded at Palestinian Territory, occupied on December 6, 2021
www.manaraa.com

In contrast to their distinct olfactory behaviors, *A. ceylanicum* and *S. stercoralis* iL3s both show robust positive thermotaxis and engage in thermosensory-driven host seeking (40). Thus, it is possible that as an alternative to oral infection, *A. ceylanicum* iL3s may elect to stay near fecal deposits, wait for mammalian hosts to arrive nearby, and then engage in thermosensory-driven host seeking to infect by skin penetration. This type of strategy, combined with the observation that *A. ceylanicum* iL3s were neutral to many of the skin and sweat odorants tested (Fig. 2 *C* and *D*), suggests that *A. ceylanicum* might achieve host specificity by detecting host-specific cues that have yet to be identified.

We note that the concentrations of many of the tested odorants in human sweat and feces are not known and likely vary significantly across individuals. The concentrations experienced by iL3s in a soil environment will depend on both distance from the host and local environmental conditions. In addition, under natural conditions, iL3s encounter these odorants as complex odor mixtures rather than individual odorants and in combination with many other sensory cues. Further studies will be necessary to determine how the iL3s respond to odor mixtures with varying concentrations of individual odorants, and, more generally, how the behaviors observed here contribute to host seeking in nature.

To identify molecular mechanisms that may be required for odor-driven host seeking in human-parasitic nematodes, we used CRISPR/Cas9-mediated targeted mutagenesis to generate *S. stercoralis* iL3s with homozygous disruptions of the *Ss-tax-4* gene (34, 40). We used *S. stercoralis* for these experiments because it is the only human-parasitic nematode that is currently amenable to genome editing. *Ss-tax-4* iL3s were unable to navigate toward the attractive host odorant 3m1b, suggesting that odor-driven host seeking in *S. stercoralis* involves a cGMP signaling pathway that includes *Ss-tax-4*. *Ss-tax-4* is also required for positive thermotaxis toward host body temperatures in *S. stercoralis* (40). Thus, *Ss-tax-4* appears to contribute to multiple aspects of sensory-driven host seeking. *Ce-tax-4* is similarly required for multiple sensory-driven behaviors in *C. elegans* (55), indicating that host seeking in parasitic nematodes and environmental navigation in free-living nematodes use signaling pathways that are at least partly conserved.

In *C. elegans*, *tax-4* is required for only a subset of olfactory responses; some olfactory responses instead require the TRPV channel *osm-9* (55). The *S. stercoralis* genome encodes an *osm-9* homolog (67), raising the possibility that some olfactory responses in *S. stercoralis* may not require *Ss-tax-4* and may, instead, require *Ss-osm-9*. Future experiments examining the responses of both *Ss-tax-4* and *Ss-osm-9* iL3s to a large panel of host-associated odorants and ethologically relevant complex odor mixtures will be necessary to address this possibility. In addition, *C. elegans* detects odorants primarily using three pairs of olfactory neurons: AWA, AWB, and AWC (55). The sensory neurons that mediate odor-driven host seeking in parasitic nematodes remain to be identified.

We found that *Ss-tax-4* is required not only for chemotaxis to a host odorant, but also for activation, suggesting that a cGMP-mediated sensory detection pathway involving *Ss-tax-4* is likely required for in-host development. These results are consistent with a previous study showing that the cGMP analog 8-bromo-cGMP stimulates activation (31). In the *C. elegans* dauer larva, a developmentally arrested life stage similar to the iL3, ASJ sensory neurons are critical for sensing environmental change and triggering resumption of development (11, 55, 68). Laser ablation studies in *S. stercoralis* iL3s showed that ASJ ablation reduced activation rates. However, approximately half of the ASJ-ablated iL3s still activated normally (14). Simultaneous ablation of the ASJ neurons and the ALD neurons, which appear to be thermosensory (39), did not further reduce activation rates (14). In contrast, *Ss-tax-4* knockout iL3s are completely unable to activate (Fig. 5*D*). Together with the fact that activation in *S. stercoralis* requires heat (37 °C), CO_2, and one or more gustatory cues present in DMEM (Fig. 5*C*), our *Ss-tax-4* results suggest that activation requires the detection of multiple sensory inputs across several sensory neuron pairs as previously proposed (14, 30, 31). Multisensory integration is presumably critical for activation to ensure that iL3s do not improperly reinitiate development outside the host. Future studies will be necessary to identify the set of sensory neurons that is required for activation.

Here, we have investigated the host-seeking strategies and chemosensory mechanisms that enable human-parasitic skin-penetrating nematodes to find and infect human hosts. Skin-penetrating nematodes are a major cause of morbidity in low-resource settings throughout the world, including some parts of the United States (2, 69). A better understanding of the chemosensory behaviors and mechanisms that contribute to the interactions of these parasites with their human hosts may allow for the development of novel approaches to preventing hookworm and threadworm infections.

Materials and Methods

All nematodes were cultured as previously described (37, 40). Host-odorant- and fecal-odor-chemotaxis assays, fecal dispersal assays, and nictation assays were performed as previously described (37, 51, 70) with modifications. The generation of *S. stercoralis* iL3s containing CRIPSR/Cas9-mediated targeted mutations and the genotyping of individual iL3s were performed essentially as previously described (34, 40). In vitro activation assays were performed as previously described (14) with modifications. Fluorescence microscopy was performed using standard methods. Statistical analysis was performed using standard statistical tests. These methods are described in detail in the *SI Appendix*, *SI Materials and Methods*. Single-iL3-odorant-chemotaxis assays are described in detail below.

Single-iL3-Odorant-Chemotaxis Assays. Wild-type, no-Cas9-control, or *Ss-tax-4* iL3s were stored in BU saline in a small watch glass prior to chemotaxis assays. A single iL3 was pipetted in 2 μL of BU saline from the watch glass and transferred to the center of a 9-cm-chemotaxis plate without odorant. The iL3 was acclimated to the chemotaxis plate for 5 min prior to the odorant assay. During the acclimation period, the iL3 was allowed to crawl freely on the agar surface. To account for any potential damage done to the animal during Baermann collection, *mRFPmars* screening, or pipetting, the iL3 had to crawl out of a 2-cm diameter circle in the center of the acclimation plate; any iL3 that failed to leave the 2-cm diameter circle during the 5-min acclimation period was discarded. iL3s that successfully navigated out of the 2-cm circle were collected at the end of the acclimation period and transferred in ∼2-μL double-distilled H_2O (ddH_2O) to the center of a 5-cm odorant-chemotaxis arena drawn in the center of a fresh 9-cm-chemotaxis plate.

For the assay, 5 μL of a 1:10 dilution of 3-methyl-1-butanol in PO and 5 μL of the PO diluent were placed 1 cm away from the iL3 on opposite sides of the arena as shown in Fig. 4*A* and *SI Appendix*, Fig. S9*A*. The plate was then placed on top of two light diffusers arranged orthogonally on a raised Plexiglas surface. The imaging surface was bottom illuminated with a white light-emitting diode (LED) box covered with a red-light filter. The entire imaging setup was placed in an opaque enclosure with the LED box as the only light source. Imaging was started immediately as the ddH_2O drop containing the iL3 dried. iL3 movements were monitored with a 5-megapixel complementary metal-oxide semiconductor (CMOS) camera (BTE-B050-U, Mightex Systems) suspended above the chemotaxis plate. Images were collected by triggering transistor–transistor logic (TTL) pulses with a USB DAQ device (U3-LV, LabJack Corp.) using a custom MATLAB script (MathWorks) (40). Images were collected for 6 min at 0.5 frames/s or until the iL3 left the 5-cm arena. Any recordings where the iL3 did not move continuously within the assay arena for at least 60 s were discarded. However, iL3s that rapidly crawled out of the assay arena in <60 s were included. iL3s were then recovered from the assay plate for single-iL3 genotyping as described below. Tracking was conducted across multiple days to control for day-to-day variability in assay conditions.

The trajectories of iL3s in the odorant arena and the locations of the odorant and control placement points were measured in Fiji using the Manual Tracking plugin (71). Custom MATLAB scripts were used to translate x/y coordinates into the tracks shown in Fig. 4 and *SI Appendix*, Fig. S9. To calculate odorant responses, each worm track was aligned relative to the x/y coordinates of the odorant placement point for that recording; tracks were rotated so that odorant and control placement points were horizontally aligned. For each assay, the experimental and control zones were defined as 1-cm diameter circles centered around the odorant or control placement points. Any iL3 that entered the experimental zone was counted as responsive to that odorant. The amount of time in seconds each iL3 spent

ECOLOGY

Downloaded at Palestinian Territory, occupied on December 6, 2021

www.manaraa.com

inside the experimental zone was determined by multiplying the number of frames in which an iL3 was found inside the experimental zone by 2. To account for directional bias, the location of the odorant stimulus was alternated between the left and the right zones for each assay. For presentation purposes, half of the tracks shown in Fig. 4 and *SI Appendix*, Fig. S9 were flipped horizontally to show the odorant in the same orientation.

Data Availability. All data and protocols are provided in the paper and *SI Appendix*. The source code is available through GitHub, https://github.com/HallemLab/Chemotaxis_Tracker.

ACKNOWLEDGMENTS. We thank Navonil Banerjee for insightful comments on the paper.

1. B. A. Boatin *et al*., A research agenda for helminth diseases of humans: Towards control and elimination. *PLoS Negl. Trop. Dis.* **6**, e1547 (2012).
2. R. L. Pullan, J. L. Smith, R. Jasrasaria, S. J. Brooker, Global numbers of infection and disease burden of soil transmitted helminth infections in 2010. *Parasit. Vectors* **7**, 37 (2014).
3. P. J. Hotez *et al*., Helminth infections: The great neglected tropical diseases. *J. Clin. Invest.* **118**, 1311–1321 (2008).
4. W. Page, J. A. Judd, R. S. Bradbury, The unique life cycle of *Strongyloides stercoralis* and implications for public health action. *Trop. Med. Infect. Dis.* **3**, 53 (2018).
5. R. J. Traub, *Ancylostoma ceylanicum*, a re-emerging but neglected parasitic zoonosis. *Int. J. Parasitol.* **43**, 1009–1015 (2013).
6. F. Schär *et al*., *Strongyloides stercoralis:* Global distribution and risk factors. *PLoS Negl. Trop. Dis.* **7**, e2288 (2013).
7. S. M. Bartsch *et al*., The global economic and health burden of human hookworm infection. *PLoS Negl. Trop. Dis.* **10**, e0004922 (2016).
8. T. W. Schafer, A. Skopic, Parasites of the small intestine. *Curr. Gastroenterol. Rep.* **8**, 312–320 (2006).
9. T. B. Nutman, Human infection with *Strongyloides stercoralis* and other related *Strongyloides* species. *Parasitology* **144**, 263–273 (2017).
10. M. Crook, The dauer hypothesis and the evolution of parasitism: 20 years on and still going strong. *Int. J. Parasitol.* **44**, 1–8 (2014).
11. P. Hotez, J. Hawdon, G. A. Schad, Hookworm larval infectivity, arrest and amphiparatenesis: The *Caenorhabditis elegans* Daf-c paradigm. *Parasitol. Today* **9**, 23–26 (1993).
12. M. E. Viney, F. J. Thompson, M. Crook, TGF-β and the evolution of nematode parasitism. *Int. J. Parasitol.* **35**, 1473–1475 (2005).
13. J. M. Hawdon, G. A. Schad, Serum-stimulated feeding *in vitro* by third-stage infective larvae of the canine hookworm *Ancylostoma caninum*. *J. Parasitol.* **76**, 394–398 (1990).
14. F. T. Ashton, X. Zhu, R. Boston, J. B. Lok, G. A. Schad, *Strongyloides stercoralis*: Amphidial neuron pair ASJ triggers significant resumption of development by infective larvae under host-mimicking *in vitro* conditions. *Exp. Parasitol.* **115**, 92–97 (2007).
15. A. J. Haley, Biology of the rat nematode *Nippostrongylus brasiliensis* (Travassos, 1914). I. Systematics, hosts and geographic distribution. *J. Parasitol.* **47**, 727–732 (1961).
16. M. E. Viney, J. B. Lok, The biology of *Strongyloides spp WormBook*, (2015), pp. 1–17. www.wormbook.org. Accessed 26 June 2020.
17. M. Viney, T. Kikuchi, *Strongyloides ratti* and *S. venezuelensis* - rodent models of *Strongyloides* infection. *Parasitology* **144**, 285–294 (2017).
18. T. J. Nolan *et al*., The sugar glider (*Petaurus breviceps*): A laboratory host for the nematode *Parastrongyloides trichosuri*. *J. Parasitol.* **93**, 1084–1089 (2007).
19. F. T. Ashton, J. Li, G. A. Schad, Chemo- and thermosensory neurons: Structure and function in animal parasitic nematodes. *Vet. Parasitol.* **84**, 297–316 (1999).
20. S. S. Gang, E. A. Hallem, Mechanisms of host seeking by parasitic nematodes. *Mol. Biochem. Parasitol.* **208**, 23–32 (2016).
21. A. S. Bryant, E. A. Hallem, Terror in the dirt: Sensory determinants of host seeking in soil-transmitted mammalian-parasitic nematodes. *Int. J. Parasitol. Drugs Drug Resist.* **8**, 496–510 (2018).
22. A. S. Bryant, E. A. Hallem, Temperature-dependent behaviors of parasitic helminths. *Neurosci. Lett.* **687**, 290–303 (2018).
23. K. Bekelaar, T. Waghorn, M. Tavendale, C. McKenzie, D. Leathwick, Carbon dioxide is an absolute requirement for exsheathment of some, but not all, abomasal nematode species. *Parasitol. Res.* **117**, 3675–3678 (2018).
24. J. M. Hawdon, S. W. Volk, D. I. Pritchard, G. A. Schad, Resumption of feeding *in vitro* by hookworm third-stage larvae: A comparative study. *J. Parasitol.* **78**, 1036–1040 (1992).
25. J. M. Hawdon, G. A. Schad, *Ancylostoma caninum*: Reduced glutathione stimulates feeding by third-stage infective larvae. *Exp. Parasitol.* **75**, 40–46 (1992).
26. J. M. Hawdon, G. A. Schad, Long-term storage of hookworm infective larvae in buffered saline solution maintains larval responsiveness to host signals. *J. Helm. Soc. Wash* **58**, 140–142 (1991).
27. S. C. C. Huang *et al*., Activation of *Nippostrongylus brasiliensis* infective larvae is regulated by a pathway distinct from the hookworm *Ancylostoma caninum*. *Int. J. Parasitol.* **40**, 1619–1628 (2010).
28. K. Bekelaar, T. Waghorn, M. Tavendale, C. McKenzie, D. Leathwick, Heat shock, but not temperature, is a biological trigger for the exsheathment of third-stage larvae of *Haemonchus contortus*. *Parasitol. Res.* **117**, 2395–2402 (2018).
29. K. Bekelaar, T. Waghorn, M. Tavendale, C. McKenzie, D. Leathwick, Abomasal nematode species differ in their *in vitro* response to exsheathment triggers. *Parasitol. Res.* **118**, 707–710 (2019).
30. J. D. Stoltzfus, H. C. Massey Jr., T. J. Nolan, S. D. Griffith, J. B. Lok, *Strongyloides stercoralis age-1*: A potential regulator of infective larval development in a parasitic nematode. *PLoS One* **7**, e38587 (2012).
31. J. D. Stoltzfus, S. M. Bart, J. B. Lok, cGMP and NHR signaling co-regulate expression of insulin-like peptides and developmental activation of infective larvae in *Strongyloides stercoralis*. *PLoS Pathog.* **10**, e1004235 (2014).
32. J. D. Ward, Rendering the intractable more tractable: Tools from *Caenorhabditis elegans* ripe for import into parasitic nematodes. *Genetics* **201**, 1279–1294 (2015).
33. J. B. Lok, H. Shao, H. C. Massey, X. Li, Transgenesis in *Strongyloides* and related parasitic nematodes: Historical perspectives, current functional genomic applications and progress towards gene disruption and editing. *Parasitology* **144**, 327–342 (2017).
34. S. S. Gang *et al*., Targeted mutagenesis in a human-parasitic nematode. *PLoS Pathog.* **13**, e1006675 (2017).
35. J. B. Lok, Strongyloides stercoralis: A model for translational research on parasitic nematode biology. *Wormbook* (2007), pp. 1–18. www.wormbook.org. Accessed 26 June 2020.
36. D. Safer, M. Brenes, S. Dunipace, G. Schad, Urocanic acid is a major chemoattractant for the skin-penetrating parasitic nematode *Strongyloides stercoralis*. *Proc. Natl. Acad. Sci. U.S.A.* **104**, 1627–1630 (2007).
37. M. L. Castelletto *et al*., Diverse host-seeking behaviors of skin-penetrating nematodes. *PLoS Pathog.* **10**, e1004305 (2014).
38. W. M. Forbes, F. T. Ashton, R. Boston, X. Zhu, G. A. Schad, Chemoattraction and chemorepulsion of *Strongyloides stercoralis* infective larvae on a sodium chloride gradient is mediated by amphidial neuron pairs ASE and ASH, respectively. *Vet. Parasitol.* **120**, 189–198 (2004).
39. P. M. Lopez, R. Boston, F. T. Ashton, G. A. Schad, The neurons of class ALD mediate thermotaxis in the parasitic nematode, *Strongyloides stercoralis*. *Int. J. Parasitol.* **30**, 1115–1121 (2000).
40. A. S. Bryant *et al*., A critical role for thermosensation in host seeking by skin-penetrating nematodes. *Curr. Biol.* **28**, 2338–2347 (2018).
41. W. M. Forbes, F. T. Ashton, R. Boston, G. A. Schad, Chemotactic behaviour of *Strongyloides stercoralis* infective larvae on a sodium chloride gradient. *Parasitology* **127**, 189–197 (2003).
42. M. Koga *et al*., Host-finding behavior of *Strongyloides stercoralis* infective larvae to sodium cation, human serum, and sweat. *Southeast Asian J. Trop. Med. Public Health* **36** (suppl. 4), 93–98 (2005).
43. Z. T. Halpin, Individual odors among mammals: Origins and functions. *Adv. Stud. Behav.* **16**, 39–70 (1986).
44. P. A. Brennan, K. M. Kendrick, Mammalian social odours: Attraction and individual recognition. *Philos. Trans. R. Soc. Lond. B Biol. Sci.* **361**, 2061–2078 (2006).
45. W. N. Grant *et al*., *Parastrongyloides trichosuri,* a nematode parasite of mammals that is uniquely suited to genetic analysis. *Int. J. Parasitol.* **36**, 453–466 (2006).
46. S. J. Stasiuk, M. J. Scott, W. N. Grant, Developmental plasticity and the evolution of parasitism in an unusual nematode, *Parastrongyloides trichosuri*. *Evodevo* **3**, 1 (2012).
47. V. L. Hunt *et al*., The genomic basis of parasitism in the *Strongyloides* clade of nematodes. *Nat. Genet.* **48**, 299–307 (2016).
48. C. I. Bargmann, E. Hartwieg, H. R. Horvitz, Odorant-selective genes and neurons mediate olfaction in *C. elegans*. *Cell* **74**, 515–527 (1993).
49. M. Blaxter, G. Koutsovoulos, The evolution of parasitism in Nematoda. *Parasitology* **142** (suppl. 1), S26–S39 (2015).
50. D. I. Grove, Human strongyloidiasis. *Adv. Parasitol.* **38**, 251–309 (1996).
51. F. Ruiz, M. L. Castelletto, S. S. Gang, E. A. Hallem, Experience-dependent olfactory behaviors of the parasitic nematode *Heligmosomoides polygyrus*. *PLoS Pathog.* **13**, e1006709 (2017).
52. T. J. Nolan, Z. Megyeri, V. M. Bhopale, G. A. Schad, *Strongyloides stercoralis:* The first rodent model for uncomplicated and hyperinfective strongyloidiasis, the Mongolian gerbil *(Meriones unguiculatus*). *J. Infect. Dis.* **168**, 1479–1484 (1993).
53. P. Garside, J. M. Behnke, *Ancylostoma ceylanicum* in the hamster: Observations on the host-parasite relationship during primary infection. *Parasitology* **98**, 283–289 (1989).
54. H. Lee *et al*., Nictation, a dispersal behavior of the nematode *Caenorhabditis elegans,* is regulated by IL2 neurons. *Nat. Neurosci.* **15**, 107–112 (2011).
55. C. I. Bargmann, Chemosensation in *C. elegans*. *WormBook* (2006), pp. 1–29. www.wormbook.org. Accessed 26 June 2020.
56. C. M. Coburn, C. I. Bargmann, A putative cyclic nucleotide-gated channel is required for sensory development and function in *C. elegans*. *Neuron* **17**, 695–706 (1996).
57. H. Komatsu, I. Mori, J. S. Rhee, N. Akaike, Y. Ohshima, Mutations in a cyclic nucleotide-gated channel lead to abnormal thermosensation and chemosensation in *C. elegans*. *Neuron* **17**, 707–718 (1996).
58. T. N. Shivakumara *et al*., Homologs of *Caenorhabditis elegans* chemosensory genes have roles in behavior and chemotaxis in the root-knot nematode *Meloidogyne incognita*. *Mol. Plant Microbe Interact.* **32**, 876–887 (2019).
59. K. Scott, Out of thin air: Sensory detection of oxygen and carbon dioxide. *Neuron* **69**, 194–202 (2011).
60. C. M. Coburn, I. Mori, Y. Ohshima, C. I. Bargmann, A cyclic nucleotide-gated channel inhibits sensory axon outgrowth in larval and adult *Caenorhabditis elegans:* A distinct pathway for maintenance of sensory axon structure. *Development* **125**, 249–258 (1998).
61. M. Ailion, J. H. Thomas, Dauer formation induced by high temperatures in *Caenorhabditis elegans*. *Genetics* **156**, 1047–1067 (2000).
62. A. Dulovic, V. Puller, A. Streit, Optimizing culture conditions for free-living stages of the nematode parasite *Strongyloides ratti*. *Exp. Parasitol.* **168**, 25–30 (2016).

Downloaded at Palestinian Territory, occupied on December 6, 2021

www.manaraa.com

63. W. Haas, Parasitic worms: Strategies of host finding, recognition and invasion. *Zoology (Jena)* **106**, 349–364 (2003).
64. W. Haas, B. Haberl, Syafruddin, I. Idris, S. Kersten, Infective larvae of the human hookworms *Necator americanus* and *Ancylostoma duodenale* differ in their orientation behaviour when crawling on surfaces. *Parasitol. Res.* **95**, 25–29 (2005).
65. W. Haas *et al*., Behavioural strategies used by the hookworms *Necator americanus* and *Ancylostoma duodenale* to find, recognize and invade the human host. *Parasitol. Res.* **95**, 30–39 (2005).
66. J. K. Landmann, P. Prociv, Experimental human infection with the dog hookworm, *Ancylostoma caninum*. *Med. J. Aust.* **178**, 69–71 (2003).
67. K. L. Howe, B. J. Bolt, M. Shafie, P. Kersey, M. Berriman, WormBase ParaSite - a comprehensive resource for helminth genomics. *Mol. Biochem. Parasitol.* **215**, 2–10 (2017).
68. C. I. Bargmann, H. R. Horvitz, Control of larval development by chemosensory neurons in *Caenorhabditis elegans*. *Science* **251**, 1243–1246 (1991).
69. M. L. McKenna *et al*., Human intestinal parasite burden and poor sanitation in rural Alabama. *Am. J. Trop. Med. Hyg.* **97**, 1623–1628 (2017).
70. J. H. Lee, A. R. Dillman, E. A. Hallem, Temperature-dependent changes in the host-seeking behaviors of parasitic nematodes. *BMC Biol.* **14**, 36 (2016).
71. J. Schindelin *et al*., Fiji: An open-source platform for biological-image analysis. *Nat. Methods* **9**, 676–682 (2012).

Downloaded at Palestinian Territory, occupied on December 6, 2021

المنارة للاستشارات
www.manaraa.com